Tomographic Image Reconstruction based on Artificial Neural Network (ANN) Techniques

M. Argyrou, P. Paschalis, D. Maintas, E. Stiliaris

Tomographic Image Reconstruction based on Artificial Neural Network (ANN) Techniques

M. Argyrou[a], P. Paschalis[a], D. Maintas[c], E. Stiliaris [1a,b]

[a]National and Kapodistrian University of Athens, Department of Physics,
Ilissia Campus, GR–15771 Athens
[b]Institute of Accelerating Systems and Applications (IASA),
P.O. Box 17214, GR–10024 Athens
[c]Institute of Isotopic Studies, Medical Center of Athens,
Distomou 5-7, GR–15125 Marousi, Athens

Abstract

A new approach for tomographic image reconstruction from projections using Artificial Neural Network (ANN) techniques is presented in this work. The design of the proposed reconstruction system is based on a simple but efficient network architecture, which best utilizes all available input information. Due to the computational complexity, which grows quadratically with the image size, the training phase of the system is characterized by relatively large CPU times. The trained network, on the contrary, is able to provide all necessary information in a quick and efficient way giving results comparable to other time consuming iterative reconstruction algorithms. The performance of the network studied with a large number of software phantoms is directly compared to the well known Algebraic Reconstruction Technique (ART). For a given image and projections size, the role of the hidden layers in the network architecture is examined and the quality dependence of the reconstructed image on the size of the geometrical patterns used in the training phase is also investigated.

1. Introduction

1.1. The Tomographic Problem

In the emission and absorbtion tomography, an image can be simply represented by a square matrix whose elements are proportional to the intensity of each pixel. Once this matrix is known, the projections in various angles θ, that is the sum of all cell contributions (Figure 1) along a certain ray R_i can be easily calculated. In tomography, we would rather interested in solving the inverse problem, that is to reconstruct the square matrix from its projections at different directions. By using the radiation emitted by an object, after the injection of radiopharmaceutical, we are able to obtain sectional (planar) images of the object. These projection data are then feeded into a reconstruction algorithm. The intensity of each ray R_i at a given angle can be calculated from the projection matrix P_{ij} and the reconstructed matrix Q_j. The projection matrix carries the information of how much the jth element of the matrix Q contributes to the ith ray. Let

---

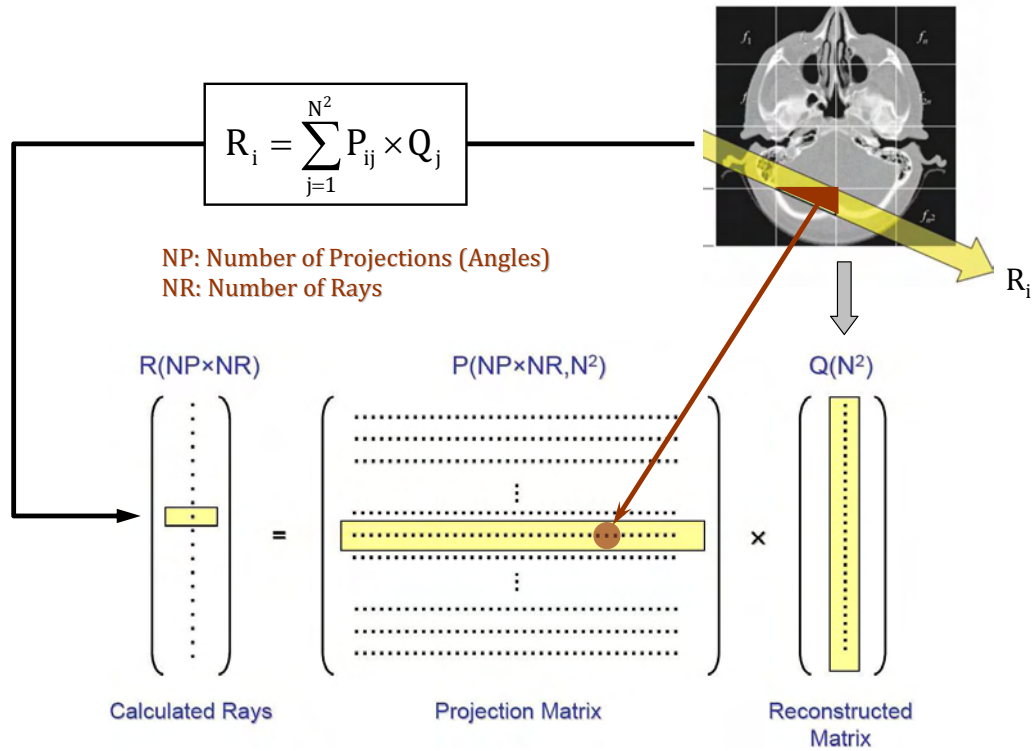[1]Corresponding author: stiliaris@phys.uoa.gr

Figure 1: Reconstruction of an $N \times N$ square matrix from its $NP \times NR$ projections.

$N \times N$ be the dimension of the square matrix, NP the number of projections (angles) and NR the number of constant width rays per each projection; then the following expression holds:

$$R_i = \sum_{j=1}^{N^2} P_{ij} \times Q_j \quad \{i = 1 \cdots NP \times NR, \; j = 1 \cdots N^2\} \tag{1}$$

1.2. Image Reconstruction Methods

In order to reconstruct an image, several solutions are proposed [1]. One of them is the use of analytic algorithms. The reconstruction can be achieved by two dimensional Fourier analysis or by the filtered back-projection. In the later, the square matrix elements are exactly calculated by solving a system with N^2 unknown and $NP \times NR$ known parameters. However, a large number of projections are required in order to obtain an exact and satisfying solution.

In the iterative procedures, random values to the square matrix elements are given initially. The projections of the matrix in different angles are calculated and the matrix elements are corrected in such a way that the calculated projections best match the measured ones. Thus, after the kth iteration the Q matrix elements are corrected as follows:

$$Q_j^k = Q_j^{k-1} + P_{ij} \frac{R_i^{meas} - R_i^{calc}}{N} \tag{2}$$

These methods, based on back-projected correction procedure, are known as Algebraic Reconstruction Techniques (ART). In a Newton-Raphson approach, an improved version of the above, the contribution of the nearest pixels and rays to the projection angles is taken into account [2]. The obtained reconstruction results are characterized by a good quality. In Figure 2 we present an example of reconstruction of a software phantom using ART. The evolution of the quantity $\chi^2 = \sum_{i=1}^{NP \times NR}(R_i^{meas} - R_i^{calc})^2$ with the number of iterations is also depicted in the same figure. The improvement of the reconstruction quality is demonstrated by the decrease of χ^2 after a sufficient number of iterations.
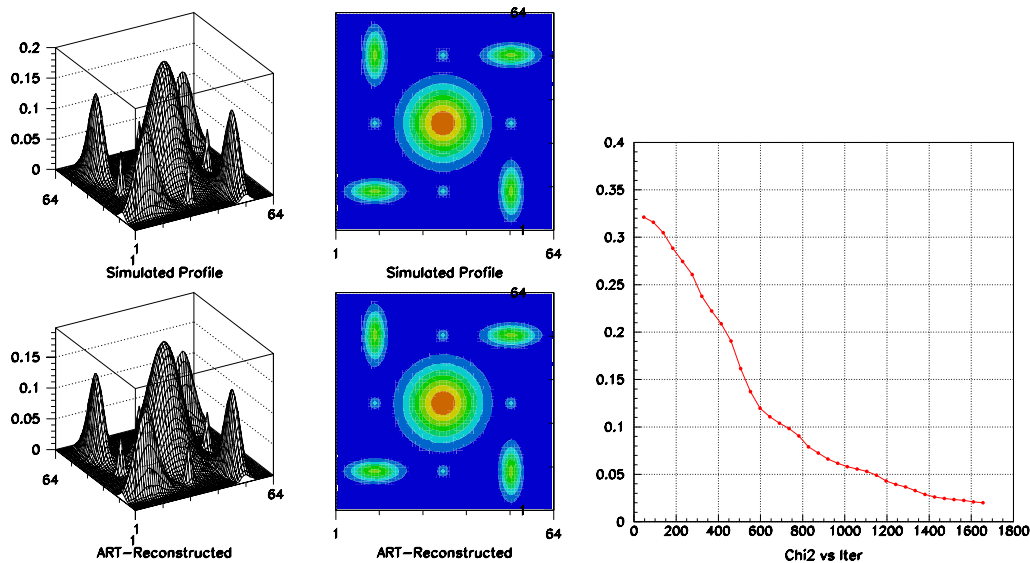

Figure 2: Reconstruction of a software phantom using ART. The original image has a dimension of $N^2 = 64 \times 64$ while the number of projections is $NP = 36$.

2. Artificial Neural Network Reconstruction

2.1. The ANN Technique

In this work we present an alternative approach to the tomographic problem using the Artificial Neural Network (ANN) Technique [3]. A typical neural network consists of the input and output layer (Figure 3). In our discussion the inputs are the experimentally obtained $NP(= M) \times NR$ projections and the outputs are the N^2 elements of the matrix to be reconstructed.

During the training process the weight factors of synapses are varied in order to approximate the desired result. This can be controlled by proper parameters, such as the learning coefficient and the momentum factor. We use the software package JETNET [4] for calculating the synaptic weight factors. It will be shown that the network architecture, and specifically the number of hidden layers, plays a crucial role in our analysis.

If no hidden layer exist and choosing for simplicity reasons $NR = N$, then the number of synapses is proportional to N^3. In the case of one hidden layer this number decreases significantly to N^2. In Figure 4 we demonstrate the reconstruction of a software phantom using ANNs with
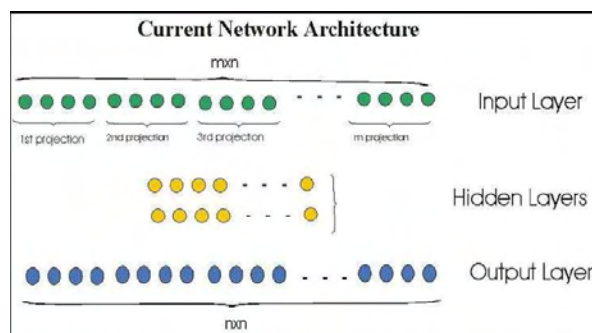
Figure 3: Architecture of the Neural Network used in the tomographic image reconstruction.

different architecture. The number of synapses in the case of no hidden layer is much larger than in the case of one hidden layer. This drastically influences the quality of the reconstructed image.

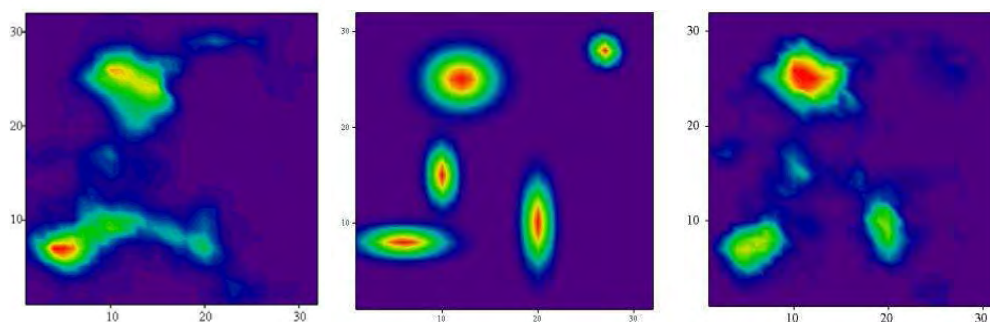| Image Size $N \times N$	Projections M	INPUT Nodes	HIDDEN Layers	OUTPUT Nodes	Synapses
32×32	18	18×32	0	32×32	589824
32×32	18	18×32	1×64	32×32	102400
32×32	18	18×32	1×32	32×32	51200

Figure 4: Reconstruction of a 32×32 software phantom (shown in the middle) with the ANN technique and for $M = 18$ projections. *Left:* One hidden layer with 64 nodes is used *Right:* No hidden layer used.

2.2. The Role of the Pattern Size

The dependence of the reconstructed image on the size of the geometrical patterns, mainly gaussian ellipsoids and parallelograms, used to construct the software phantom ensemble is discussed here. Three different phantom groups are generated containing geometrical patterns randomly distributed with various widths, which are controlled by the parameter σ and are also randomly distributed between predefined limits. Each of these phantom ensembles is further used as training input for the ANN reconstruction procedure. Data for $N^2 = 64 \times 64$ images are generated with $M = 18$ projections. These image groups trained separately the three different

ANN schemes, each one corresponding to a given pattern size. All three ANN have identical architecture but no hidden layers. The successfully trained networks are finally checked with control images.

Following this procedure, we can tabulate the reconstructed results in a form of a 3×3 matrix for an easier understanding, as shown in the following table. Each row corresponds to a different control image and each column to a specific ANN type, which is trained with a different pattern size. For example, the image A_{ij} is the reconstruction result of the original control image C_i (generated with pattern-width σ_i) produced by the network trained with pattern-width σ_j.

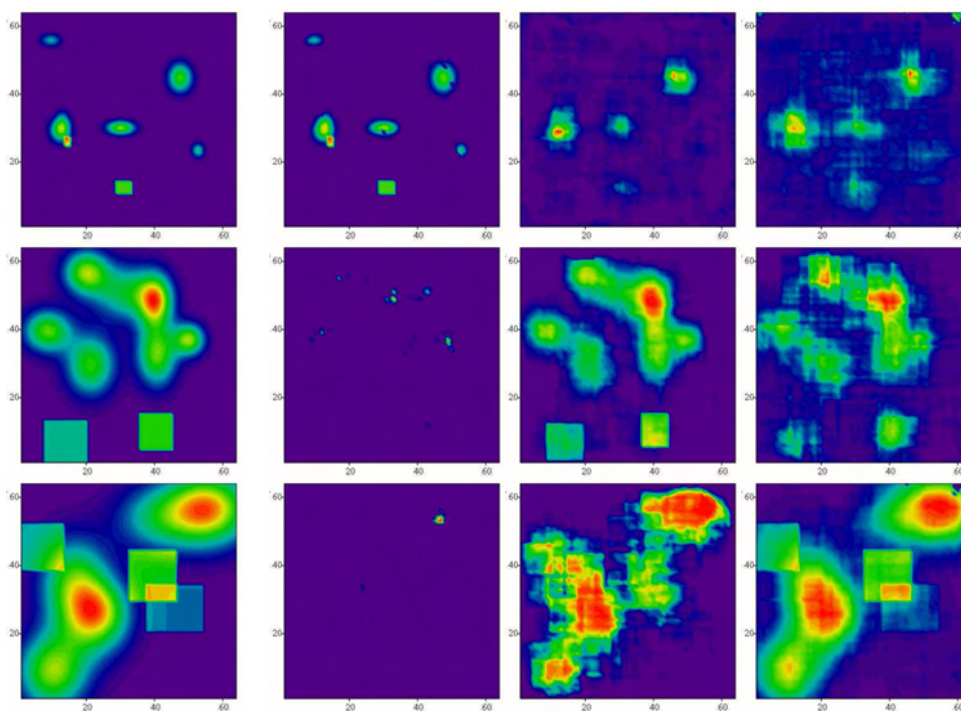| Control Images	Reconstructed Images		
C_1 ($1.0 < \sigma_1 < 3.0$)	A_{11}	A_{12}	A_{13}
C_2 ($3.0 < \sigma_2 < 6.0$)	A_{21}	A_{22}	A_{23}
C_3 ($6.0 < \sigma_3 < 9.0$)	A_{31}	A_{32}	A_{33}

Figure 5: Reconstruction of control images with differently trained ANNs, as explained in the previous table. The original control images are shown on the left panel and the reconstructed ones on the right.

Results of these control images are shown in Figure 5. As expected, the best reconstruction quality is obtained for the diagonal elements of the matrix, that is for the reconstruction by the ANN trained with the same patterns as those of the original control image. On the contrary, the reconstruction result provided by ANN trained with smaller σ-parameters than the control images, fails totally.

3. Concluding Remarks

We have presented a technique based on the Artificial Neural Networks, which is alternative to known analytic and iterative methods (ART). The main disadvantage is the large CPU time and memory requirements during the training process. However, after the training, one can obtain reliable results in a quick and efficient way. It is shown that the network architecture can affect the quality of the reconstructed image. The best results are obtained with no hidden layers. Finally, the reconstruction quality strongly depends on the size of the geometrical patterns used in the training phase. It is preferable to reconstruct images using an ANN trained with patterns of comparable size with the required spatial resolution.

References

[1] T.M. Buzug, *"Computed Tomography"*, Springer-Verlag, Berlin (2008) ISBN: 978-3-540-39407-5.

[2] S. Angeli and E. Stiliaris, *"An Accelerated Algebraic Reconstruction Technique based on the Newton–Raphson Scheme"*, IEEE NSS-MIC (2009) 3382–3387.

[3] P. Paschalis *et al.*, *Tomographic image reconstruction using Artificial Neural Networks*, Nucl. Instr. and Meth. **A 527** (2004) 211–215.

[4] C. Peterson, Th. Rögnvaldsson, L. Lönnblad, *"JETNET 3.0 - A versatile artificial network package*, Comp. Phys. Comm. 81 (1994) 185–220.